Large-Angle Collisions in an Aluminum Surface Bombarded by 50-keV Argon Ions*

POUL DAHL† AND JOHN MAGYAR‡
Physics Department, University of Connecticut, Storrs, Connecticut

(Received 16 April 1965; revised manuscript received 16 July 1965)

The ejection of charged atomic particles from the surface of an Al target during irradiation by 50-keV Ar^+ ions was studied. At several angles to the incident beam an analysis of emitted ions was performed by electrostatic deflection to a single-particle detector. The spectra show sharp peaks superimposed on a continuum. The peaks correspond to single collisions. From accurate measurements of peak positions, the inelastic energy loss in the Ar on Al collisions is obtained by methods assuming pure single collisions. The values are about 450 eV for the Al recoil peaks at angles from 77° to 50°, and higher values (up to 600 eV) are found for more violent collisions. Variation of the angle which the surface forms to the incident beam did not influence the peak positions. This result supports the single-collision assumption. Absolute measurements of spectral intensities were also performed, and the number of target atoms per cm^2 that would account for the measured peak intensities was derived by applying generally accepted theoretical scattering cross sections. Typically, single-collision scattering is obtained from target atoms with density comparable to or less than the density in a {100} crystal plane. Theoretical estimates of multiple scattering are used in a discussion of the peak formation. The target was a single crystal, but the surface included an oxygen impurity, and no lattice-directional effect was observed. The continuum is interpreted; the discussion is based on the absolute intensity measurements and on the theory for penetration of heavy ions in the keV region for random distribution of target atoms.

I. INTRODUCTION

IRRADIATION of the surface of a solid by energetic atomic particles causes emission of ions both of the target element and of the incident particles. The emission from Cu, Ag, and Au during bombardment by Ar^+ ions (40–80 keV) was investigated by Datz and Snoek[1]. Magnetic analysis of the emission in various directions was performed, and the spectra showed sharp peaks at positions in agreement with the kinematics of a single collision between an incident ion and a free target atom. Peaks corresponding to various charge states of the ejected ions were found, and the existence of highly charged ions is ascribed to the violence of the collision. It was pointed out that solid targets may be used in single-collision studies.

The present paper describes a similar investigation in which 50-keV Ar^+ ions are incident on an Al target. Spectrum peaks corresponding to single collisions are found superimposed on a continuum which, in this case, turns out to form the main part of the spectrum.

Our concern in a single-collision study should be the multi-ionization process which has been the subject for a number of investigations using gaseous targets, in particular the measurements reported by Everhart and his collaborators,[2] and by Fedorenko and his collaborators.[3] In these experiments are measured probabilities for the various charge states of the ions produced, and the inelastic energy given off to electrons in violent collisions. The inelastic energy loss can be obtained from accurate measurements of scattering angles and particle energies, by methods described by Morgan and Everhart.[2] It was found by Morgan and Everhart that the energy loss is related first to the distance of closest approach. The inelastic energy loss is high (several hundred eV), and highly charged ions are produced, when inner shells of the colliding atoms are overlapping during the collision. A theory developed by Russek[4] describes the multi-ionization as a two-step process—first the high inelastic energy is stored as compound excitation of inner shells which later decay by autoionization transitions.

For particles ejected from the surface of a solid, the spectrum peaks are ascribed to single collisions, but the distribution of charge states might not be the same as for single collisions with free atoms. We shall first be concerned with the inelastic energy loss because when dealing with violent collisions, a major part of the energy loss should be ascribed to interior parts of the atomic particles. A problem in the use of a solid target is to what degree the measurement is disturbed by weak secondary collisions with surrounding atoms in the target surface. It is therefore investigated whether the peak positions, from which the inelastic energy is obtained, depend only on the scattering angle and not on the angle the target surface makes with the incident beam.

In order to explain the spectra, as they appear with peaks superimposed on a continuum, we should be concerned with the multiple-collision phenomena. One question, which is of interest also for the above-

* This work was supported by the U. S. Army Research Office, Durham.

† On leave from: Institute of Physics, University of Aarhus, Aarhus, Denmark.

‡ Present address: Department of Physics and Astrophysics, University of Colorado, Boulder, Colorado.

[1] S. Datz and C. Snoek, Phys. Rev. **134**, A347 (1964).

[2] G. H. Morgan and E. Everhart, Phys. Rev. **128**, 667 (1962).

[3] V. V. Afrosimov and N. V. Fedorenko, Zh. Tekhn. Fiz. **27**, 2557 (1957) [English transl.: Soviet Phys.—Tech. Phys. **2**, 2378 (1957)].

[4] A. Russek, Phys. Rev. **132**, 246 (1963).

mentioned problem, is: What is the number of atomic layers from which the ejection of particles appear as being caused by single collisions? In order to examine this question, absolute measurements of the peak intensities must be performed, and this involves measurements of the particle intensity in each beam, and an analysis of the geometry of the apparatus. It is then possible to derive the number of target atoms contributing to single-collision scattering, because theoretical cross sections are available for scattering in single collisions between atomic particles.

The explanation of the existence of peaks on top of a continuum, and of the shape of the continuum, involves large-angle single collisions below the surface, and penetration phenomena such as stopping and multiple scattering. The absolute intensity measurement, and the theory for heavy-ion penetration given by Lindhard *et al.*,[5] forms a basis for discussion.

The paper is divided into seven sections. Section II describes the apparatus, and in Sec. III, the data are presented. Section IV deals with the inelastic energy loss in single collisions, and Sec. V with the number of atomic layers in the target surface from which single-collision scattering is obtained. In Sec. VI an interpretation of the spectra and a discussion of this interpretation are given. Section VII forms a conclusion.

II. APPARATUS

The Ar^+ ion beam was produced by the University of Connecticut heavy-ion accelerator. The scattering apparatus had an electrostatic analyzer followed by a secondary electron multiplier used as a single-particle detector. This apparatus had been used in previous investigations with gaseous targets. The gas-target cell was replaced by the aluminum target situated in a Faraday cage with a narrow slot from which ejected particles could emerge towards the analyzer. In this way, continuous recording of the intensity of the incident beam was performed.

Figure 1 shows the apparatus. The Ar^+ beam is steered through the collimator holes a and b, diameter 0.51 mm (area 2.0×10^{-3} cm^2), and 127 mm apart. The irradiated target surface is a plane containing the normal to the beam-analyzer plane. The target can be rotated about this normal for choosing the angle ψ of beam incidence. The target surface should contain the scattering center defined by the collimator axis and the axis of the entrance to the analyzer, and to perform this adjustment, the Faraday cage with target is moveable. Further, the target can be pulled out of the beam which then goes through the slot in the cage.

The range of the analyzer angle Φ is 0°–100°. The analyzer entrance is a two-slit system, c and d. Slit c is 0.094 mm wide, and slit d 0.24 mm; they are 70 mm apart. Thus, the angular range accepted by the slit-slit

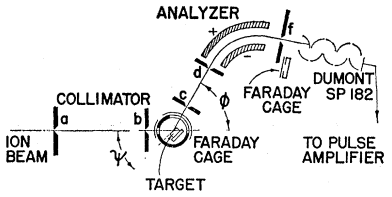

FIG. 1. The scattering apparatus (not drawn to scale).

system is $\Delta\Phi=0.27°$. The distance from the scattering center to slit c is 16 mm. The transmission angle u in the plane perpendicular to the beam-analyzer plane is limited, by the length of slit d, to $u=1.0°$. The electrostatic analyzer has the deflection angle 72° and radius 63.5 mm.

In the scattering analysis, those ions, which by deflection in the analyzer are brought through slit f, are counted individually by the secondary electron multiplier.

Calibration of the analyzer was made at $\Phi=0°$ with target pulled out of the 50-keV Ar^+ ion beam, and in this case a Faraday cage was put behind slit f. The calibration was reproducible within 0.05%.

The slit f is 0.86 mm wide, and the dispersion of the analyzer makes this slit width corresponding to a 1.62% energy interval for ions having a particular charge number; this was measured on the direct Ar^+ beam at $\Phi=0°$. The distances from slit c to the analyzer and from the analyzer to slit f are chosen so that particles having the same energy per charge unit will form a very small image of c on f. We may consider ions having the same energy-to-charge ratio as being focused at slit f.

Besides calibration of the analyzer, the measurements on the direct beam were used for adjustments of the incident beam which should be an aligned parallel beam. The current to the front button of the collimator is measured, and only a minor fraction of the beam passes through hole a; we may thus assume a uniform current density. Further, an aligned parallel beam is limited to a known fraction by slit c. It was possible to obtain a parallel beam with a current density about 10 μA/cm^2. We had normal vacuum conditions, and the beam intensity was not sufficient for removing all oxygen from the surface.

It should be mentioned that the Al target was a single crystal. The bombarded surface was a {100} plane, having a ⟨100⟩ axis in the surface lying in the beam-analyzer plane. We did not, however, find effects which we would ascribe to the crystal structure. This may be surprising because Datz and Snoek[1] found for the Cu crystal that the background in the spectra (the continuum) was clearly reduced when the crystal was bombarded with beam incidence along a [110] direction. The group in Amsterdam has later shown that the surface must be clean; the effect is not seen when strong oxygen peaks are found in the spectra.

[5] J. Lindhard, M. Scharff, and H. E. Schiøtt, Kgl. Danske Vidensk. Selskab, Mat. Fys. Medd. 33, No. 14 (1963).

III. DATA

Spectra were taken at angles Φ in the range 10° to 100° with various angles ψ of beam incidence. Figure 2 shows spectra taken at $\Phi=50°$ with $\psi=45°$, 25°, and 5°, and Fig. 3 shows a spectrum taken at $\Phi=25°$ with $\psi=22°$. The abscissa is the energy-to-charge ratio E/n and the ordinate is the normalized spectral intensity which is obtained from the count rate n_c as

$$J_n=n_c/(0.0162\times E/n). \quad (1)$$

It is seen that J_n is the count rate per unit E/n, because 0.0162 E/n is the analyzer window defined by slit f.

Peak positions were reproducible in all spectra within the accuracy of measurements. Here, a peak position is determined from the top point of the peak after subtraction of the continuum. Peak area taken as peak height times half-peak width was reproducible within ±15%, while the peak shape varied, especially the shape of peak wings. The continuum intensity was reproducible within ±15%, and the variations are not correlated in a simple manner to the variations of peak intensities. At small angles of beam incidence ($\psi\lesssim 5°$), intensity variations were larger and often took place during recording of a spectrum.

Peaks are identified by the kinematics of single collisions. Let us consider a collision where an Ar^+ ion with incident energy 50 keV hits a free Al atom at rest, and let us assume that the collision is elastic. The conservation of energy and momentum determines the energy of the scattered Ar ion as a function of the scattering angle, and the energy of the Al recoil as a function of the recoil angle. These functions, marked Ar and Al, respectively, are shown in the upper part of Fig. 4. The maximum scattering angle for Ar is 42.5°.

For the Ar on Al collision, the peaks that show up clearest are the Al^{2+} and Al^{3+} peaks, and they are found in a wide Φ-range, 25° to 77°. For the Al^+ peak, the continuum substraction is uncertain. Peaks corresponding to Al^{n+} with $n>3$ are not found. The Ar^{2+} peak is found at $\Phi=25°$ and 30°. Also, the Ar^+ peak exists, but continuum subtraction is uncertain. Peaks corresponding to Ar^{n+} with $n>2$ are not found.

Evidently, the surface included an oxygen impurity, because peaks are found which were identified as caused by argon on oxygen collisions. The maximum scattering angle in these collisions is 23°. In spectra taken at smaller angles, Ar scattered from oxygen is seen as strong Ar^+, Ar^{2+}, Ar^{3+}, and Ar^{4+} peaks, which is unlike the data for the Ar on Al collision where the high charge number peaks for Ar were not found; this discrepancy is discussed in Sec. VI.1. Oxygen recoils are seen as an O^+ peak, Figs. 2 and 3, and it is noted that only the O^+ peak exists. Also, a hydrogen impurity is present which is seen as a peak identified as H^+ recoils, Fig. 3.

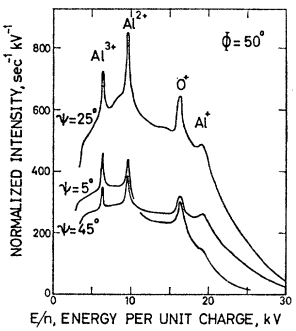

FIG. 2. Spectra taken at angle $\Phi=50°$ with $\psi=45°$, 25°, and 5°.

The irradiation must induce an Ar contamination, but if Ar atoms are exposed at the surface by removal of overlayers through sputtering, the Ar atoms evaporate immediately, leaving almost no Ar in the top surface layer. No peaks caused by Ar on Ar collisions are found; this is in accord with Ref. 1. (We may mention, though, that the dent to the right of the Al^{3+} peak in Fig. 3 could be Ar^{3+} scattered from Ar.)

In the $\Phi=50°$ spectra, Fig. 2, the continuum intensity drops off at the position for the Al^+ peak, and the tail at higher E/n ratios is a minor fraction of the continuum. The tail becomes more dominating at larger

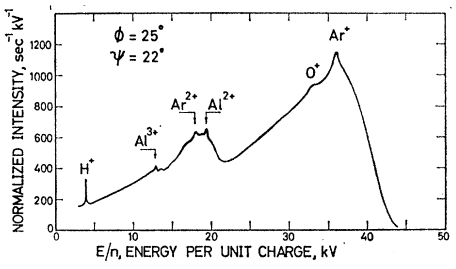

FIG. 3. Spectrum taken at angle $\Phi=25°$ with $\psi=22°$.

Φ angles, and for $\Phi\gtrsim 65°$, the main part of the continuum is found above the Al^+ peak position.

IV. INELASTIC ENERGY LOSS IN SINGLE COLLISIONS

1. Theory of Measurements

For an inelastic collision between an incident ion and a free target atom at rest, the energy of the recoil, or of the scattered particle, at a particular angle is slightly different from the energy calculated for the elastic collision. The inelastic energy loss can be obtained by using the conservation equations for energy and momentum where the total momentum of detached electrons is neglected. Let T_0 be the energy of the incident ion; energy and angle of the scattered particle are T_1 and Θ, and energy and angle for the recoil are T_2 and φ. The mass of the incident ion is M_1, and the mass of the target atom is M_2. The inelastic energy Q can be obtained from measurement of (T_0,T_1,Θ) or of

(T_0,T_2,φ), and is given by

$$Q(T_0,T_1,\Theta)=\frac{2M_1}{M_2}(T_0T_1)^{1/2}\times\cos\Theta-\frac{M_1+M_2}{M_2}T_1-\frac{M_1-M_2}{M_2}T_0 \quad (2)$$

or by

$$Q(T_0,T_2\varphi)=2\left(\frac{M_2T_0T_2}{M_1}\right)^{1/2}\cos\varphi-\frac{M_1+M_2}{M_1}T_2. \quad (3)$$

We want to plot the Q values versus the closest approach r_0 between the atomic centers during the collision, where r_0 depends on the interatomic potential. For the screened Coulomb potential suggested by Bohr, calculations by Everhart[6] are available.

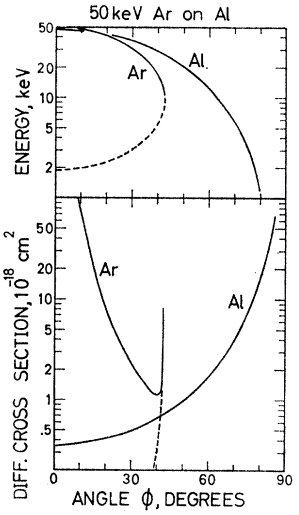

FIG. 4. The curve marked Ar in the upper part of the figure shows kinetic energy T_1 of Ar scattered in an elastic 50-keV Ar^+-on-Al collision as a function of scattering angle, Θ, $(\Theta=\Phi)$. The curve marked Al is kinetic energy T_2 of the Al recoil as a function of recoil angle $\varphi(\varphi=\Phi)$. Below is shown the corresponding cross sections $d\sigma/d\omega$ derived from the theory given by Lindhard *et al.* (Ref. 5).

As to resolving power in the experiment, we should consider the analyzer window defined by slit f (1.62%), and the energy spread due to the range in scattering angle (or recoil angle) which is defined by slit c and slit d ($\Delta\Phi=0.27°$). This energy spread may be calculated for elastic collisions, and for Ar on Al it is found to be smaller than the 1.62% window when the recoil angle is smaller than 59°, or when the scattering angle is smaller than 36°; in these cases the resolving power is determined first by the analyzer window.

2. Results

Figure 5 shows the Q values for the Ar on Al collisions plotted versus Φ and versus r_0. The plot versus r_0 shows that the values obtained from the recoil peaks, Al^{2+} and Al^{3+}, are in agreement with the values obtained from the Ar^{2+} peak. The discrepancy for the Ar^+ peak data may be ascribed to uncertainty in continuum subtraction. The inelastic energy obtained from the Al^{2+} peak seems to be lower than the value from the Al^{3+} peak, but the difference is hardly significant.

[6] E. Everhart, G. Stone, and R. J. Carbone, Phys. Rev. 99, 1287 (1955).

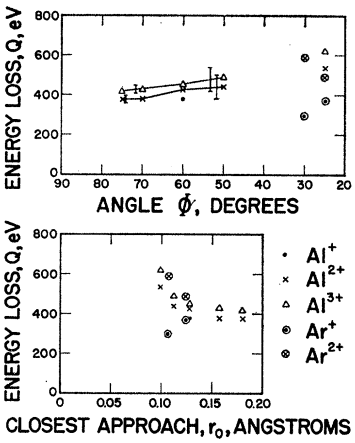

FIG. 5. The inelastic energy loss Q derived from Al and Ar peaks in the spectra plotted in the upper figure versus the angles Φ at which the spectra were taken, and below plotted versus closest approach r_0, between the atomic centers during the collisions. Here, r_0 is obtained from tabulated calculations by Everhart *et al.* (Ref. 6).

It is seen that the measured Q values are about 450 eV for values of r_0 in the interval from 0.12 to 0.18 Å, and higher values for r_0 approaching 0.10 Å. It may be interesting to compare the Q values obtained here for the Ar on Al collision to Morgan and Everhart's results for the Ar on Ar collision. They found an inelastic energy about 700 eV at the values of r_0 considered here, and it is noted that the Q values obtained for the Ar on Al collision is of the same order of magnitude.

In order to perform a check on the assumption that the inelastic energy measured here can be ascribed to the single collision, it was investigated whether the result depends on the angle of beam incidence ψ or not. The check was performed especially for the Al^{2+} and Al^{3+} peaks in spectra taken at $\Phi=50°$, and the assumption was confirmed as it was found that Q was a constant in most of the available interval for ψ, 5° to 45° (outside this interval the amount of data is not sufficient for a definite answer).

Typical values of half-peak width (full-width at half-maximum) are for the Al^{2+} peaks 4.3% at $\Phi=50°$, and 11.5% at 70°, and for the Al^{3+} peaks 3.3% at 50°, and 8.5% at 70°. In all cases, the difference between the energy-to-charge ratio for the peak top point and the ratio calculated for an elastic collision is of the same order of magnitude as the half-peak width.

We have put the main emphasis on the Ar on Al collision, but it shall be mentioned also that the inelastic energy loss for the argon on oxygen collision as deduced from the O^+ peak is about 400 eV.

V. NUMBER OF TARGET ATOMS FOR SINGLE-COLLISION SCATTERING

1. Theory of Measurement

In the lower part of Fig. 4 is shown the differential cross sections $d\sigma/d\omega$ in the 50-keV Ar-on-Al collision for scattering of Ar at angle $\Theta=\Phi$, and for getting an Al

recoil at angle $\varphi=\Phi$. The cross sections are derived from Lindhard's theory based on an interatomic potential obtained from a Thomas-Fermi treatment. These cross sections are used for obtaining the number of target atoms from which single collisions, as evident from the spectrum peaks, account for the particle ejection.

Let us first consider a single peak, for instance an Al^{2+} peak in a spectrum taken at analyzing angle Φ. We want now to derive the number of target atoms per cm^2 which would account for the intensity of the peak if all Al recoils from single collisions were doubly charged. We shall express this number as a number of atomic layers $N(Al^{2+})$, where the density in one layer is $\eta=1.22\times10^{15}$ Al atoms per cm^2; it is noted that η is the density of Al atoms in a {100} plane, and thus the distance between layers is half of the lattice constant. The number $N(Al^{2+})$ shall then be used as an absolute measure of the peak intensity.

The number of Al atoms per cm^2 for the Al^{2+} peak is $\eta\, N(Al^{2+})$, and this times $d\sigma/d\omega$ for Al recoils at $\varphi=\Phi$ will give us the probability per solid angle unit, $dP(Al^{2+})/d\omega$, that one incoming Ar^+ ion causes ejections of an Al^{2+} ion contributing to the peak. Thus we have, for each peak, an equation

$$dP/d\omega=\eta N(d\sigma/d\omega). \tag{4}$$

Here $dP/d\omega$ can be obtained from the data as

$$dP/d\omega=I/iG, \tag{5}$$

where I is the recorded peak intensity per sec of gate time, i is the number of incoming Ar^+ ions per sec and per cm^2 of the irradiated target surface, and G is the irradiated area times the solid angle through the slit-slit system to the analyzer. The quantity G may be called the geometrical transmission.

The peak intensity I is the peak area in the normalized spectrum. Because of variations in the shape of peak wings, we shall insert for I the peak height times half-peak width.

From the measured current j to the target i is obtained as

$$i=(j/e)\sin\psi/(2.0\times10^{-3}), \tag{6}$$

where 2.0×10^{-3} was the beam cross section in cm^2.

The geometrical transmission G has been calculated for the various combinations of Φ and ψ. The expression used in the calculation is

$$G=\int_{\Delta\Phi} A(\Phi')u\,d\Phi', \tag{7}$$

where $A(\Phi')$ is the irradiated area from which ions ejected into direction Φ' will get through slit c and slit d, and u, as mentioned in Sec. 2, is the transmission angle in plane perpendicular to the beam-analyzer plane.

From Eqs. (4) and (5) it follows that N is given by

$$N=I/(iG\eta d\sigma/d\omega). \tag{8}$$

The number of atomic layers from which Al recoils are identified as due to single collisions may be found as $\sum_n N(Al^{n+})$.

2. Results

The peak intensities expressed as the number N introduced in Sec. 5.1 are listed in Table I. The intensity of the oxygen peak $N(O^+)$ is obtained in a parallel manner as in reducing the Ar^+ on Al data, here using cross sections for the argon on oxygen collision; $\eta=1.22\times10^{15}$ cm^2 is again used as atom density in a layer. The summation $\sum N$, given in the $\Phi=50°$ cases, includes $N(O^+)$.

The intensity ratio $N(Al^{2+})/N(Al^{3+})$ is decreasing with decreasing recoil angle φ in a region around 50°. It may be mentioned also that this ratio does not depend sensitively on the angle ψ of beam incidence.

In the case with $(\Phi,\psi)=(50°,25°)$ it is seen that the number of target atoms for single-collision scattering corresponds to about one atomic layer, or rather less than one layer. Of the three cases, $\psi=45°$, 25°, and 5°, the $\psi=25°$ case is the more clear-cut because the unknown surface roughness is of importance when the incoming or the outgoing beam forms a small angle to the surface. When angle ψ is close to Φ, the number $\sum N$ is small which may be due to roughness making only part of the surface visible from the analyzer. It seems like ejection, apparently caused by single collisions, is favored by a large angle between the recoil direction and the surface; this possibly indicates that multiple scattering of the incident Ar^+ ion is of minor importance.

When the recoil angle is increasing from 70° to 77°, it corresponds to the recoil energy decreasing from about 5 to 2 keV, and as seen from Table I, the peak intensities approach zero. This may be due to electron capture neutralizing the recoils.

VI. INTERPRETATION OF THE SPECTRA

1. Qualitative Interpretation

In this section, we shall explain the spectra and arrive at a qualitative description of the collision phenomena causing the particle ejection. This description is

TABLE I. Peak intensities expressed as the number N of atomic layers (with atom density as a {100} plane) in the target surface, contributing to the particular peaks. For instance, $N(Al^{2+})$ is the number of layers which would account for the spectrum intensity of the Al^{2+} peak if all the Al recoils from single collisions were doubly charged.

Φ	77°–70°	70°–54°	54°–45°	50°	50°	50°	25°
ψ	45°	45°	45°	45°	25°	5°	22°
$N(Al^+)$				(0.03)	(0.14)	(0.2)	
$N(O^+)$	0–0.11	0.11	0.11–0	0.054	0.34	(1.0)	
$N(Al^{2+})$	0–0.10	0.10	0.10 –0	0.027	0.20	(0.8)	(0.075)
$N(Al^{3+})$	0–0.025	0.025	0.025–0	0.013	0.09	0.54	(0.06)
$N(Ar^{2+})$							0.01
			ΣN	0.12	0.77	2.5	

justified or made plausible by estimates, given in Sec. 6.2, based on Lindhard's theory for heavy-ion penetration.

A characteristic feature of the spectrum is that it may be divided into a continuum and the peaks. The peaks are identified, but the continuum is a superposition of unresolved partial spectra for the possible particle types Al^+, Al^{2+}, Ar^+, etc. The partial spectrum for an ion group with charge number n is not an energy spectrum with spectral intensity J plotted versus energy E, but a J'-versus E/n-spectrum, where $J'=nJ$.

The desirable basis for an understanding of the particle ejection would be the energy spectrum of the target particles and of the reflected Ar ions, regardless of charge number. We shall therefore first consider cases where we may form some ideas about the particle types in the continuum. We assume that the particle ejection seen as the continuum is caused by multiple collisions. Let us first consider the simplest case, which is well known for very high energies of the incident particles. Here, large-angle collisions are rare so that ejection of a particle is caused by only one violent collision in or below the surface. The incident and the outgoing particle are both slowed down as they penetrate target material, but without deflections; the energy spectrum will then have an edge because a maximum energy is obtained from collisions in the surface. We shall refer to that case as "the one-deflection model" (also when the ejected particle is the recoil). The model may eventually apply as a rough approximation in our experiment when considering spectra taken at angles where the involved single collision is a violent one, that is at small angles for recoils. Furthermore, a simplification results from the fact that there is a maximum scattering angle in Ar on Al collisions, $\Theta_{max}=42.5°$, which means that, if the one-deflection model applies, there will be no Ar groups in a spectrum taken at a larger angle. For these reasons, we shall first try to explain the spectra taken at $\Phi=50°$, Fig. 2.

It is seen that the continuum in the $\Phi=50°$ spectra really drops off at the position for the Al^+ peak, but it does not have a sharp edge. Thus, the one-deflection model only roughly describes the particle ejection. As a further interpretation, we shall state that the major part of the Al recoils are ejected as Al^+ ions, which is consistent with the shape of the continuum. We may then make use of the absolute intensity measurement which in Sec. VI.2B is compared to the spectral intensity deduced from the one-deflection model. As seen from the high-energy tail, the model can only yield a rough description, and it does not predict the existence of a peak corresponding to single collisions. Thus, we have to modify the model, taking multiple scattering into account for violent collisions below the surface. A theoretical estimate given in Sec. VI.2C confirms that multiple scattering gives rise to angular straggling which, though sufficient for accounting for the high-energy tail, is still small enough for justifying that the one-deflection model yields an estimate of the continuum height. The peak formation is discussed in Sec. VI.2D.

We shall now consider the $\Phi=25°$ spectrum, Fig. 3. The shape of the continuum indicates that there are two partial spectra, one having an edge at the position for the Ar^+ peak, and the other having an edge at the Al^{2+} peak. The two apparent groups might not be pure partial spectra, but let us identify them as Ar^+ ions and Al^{2+} ions, respectively. The particle ejection is ascribed to one-deflection processes. It is noted that the spectral intensity in the Ar^+ group is decreasing for decreasing energy, and this, as shall be seen below (Secs. VI.2A and VI.2B), is not consistent with the stopping theory if all reflected Ar ions escape as singly charged ions. We may suggest that a fraction, which is increasing towards lower energies, is ejected as neutrals. In parallel to this it is noted that the peak data, Sec. V.2, show very few Ar ions from single collisions with high charge numbers. Presumably, highly charged Ar ions do result from the violent collision with close approach and high Q value, Sec. IV.2, and the absence of the corresponding peaks is ascribed to electron capture. It is noted, Sec. III, that peaks for Ar^+, Ar^{2+}, Ar^{3+}, and Ar^{4+} scattered in argon on oxygen collisions, were found in spectra taken at angles smaller than the maximum scattering angle 23°. The discrepancy between data for Ar scattered from Al and for Ar scattered from oxygen could be explained if the oxygen impurity was an adsorbed layer. *A priori* one might rather expect an Al_2O_3 layer, so the effect is a bit peculiar. In the theoretical estimate of the continuum height we shall use stopping-power values for slowing down in Al.

2. Theoretical Estimates

A. Stopping Power

In Lindhard's theory, the stopping power is the sum of the nuclear stopping (recoil energies transferred to atoms) and the electronic stopping. Lindhard introduces dimensionless measures ρ and ϵ of range and energy, and a consequence of the Thomas-Fermi treatment is that the nuclear stopping S_n in ρ-ϵ variables is obtained as the same function of $\epsilon^{1/2}$ for all ion-target combinations. The electronic stopping is $S_e=k\,\epsilon^{1/2}$, where the constant k depends on Z_1 and Z_2. In Fig. 6 is shown the universal function $S_n(\epsilon^{1/2})$, and $S_e(\epsilon^{1/2})$ is shown for Al through Al where $k=0.14$. For Ar through Al, we have $k=0.12$. The theoretical stopping power in ρ-ϵ variables $d\epsilon/d\rho$ is the sum of $S_n(\epsilon^{1/2})$ and $S_e(\epsilon^{1/2})$.

The energy of the Al recoil from a 50-keV Ar-on-Al collision is $T_2=19.3$ keV at recoil angle $\varphi=50°$. The value of $\epsilon^{1/2}$ for 19.3-keV Al-through-Al is $\epsilon^{1/2}=0.74$, and it is seen from Fig. 6 that $d\epsilon/d\rho$ is almost constant down to, say, $\epsilon^{1/2}=\frac{1}{2}\times 0.74$, corresponding to $E=\frac{1}{4}T_2\approx 5$ keV. The stopping power for Al through Al in this energy region is $(dE/dR)_{Al}=0.064$ keV/Å.

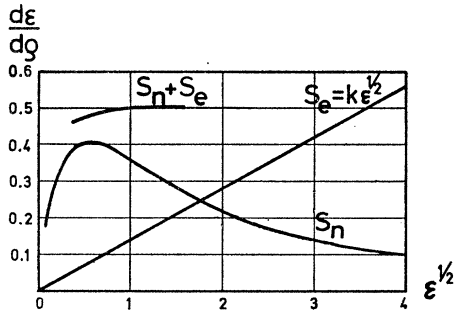

FIG. 6. The variables ρ and ϵ are the dimensionless measures of range and energy introduced by Lindhard (Ref. 5), and the figure shows the curve $S_n(\epsilon^{1/2})$ for nuclear stopping, which applies to all ion-target combinations, and the electronic stopping for Al in Al, $S_e=k\,\epsilon^{1/2}$ with $k=0.14$. The total stopping power is $d\epsilon/d\rho=S_n+S_e$.

For 50-keV Ar-on-Al it is found that $\epsilon^{1/2}=0.90$, and $d\epsilon/d\rho$ is constant in region down to low energies. The stopping power for Ar through Al is $(dE/dR)_{\mathrm{Ar}}=0.10$ keV/Å.

B. Continuum Height Compared to the Spectral Intensity Deduced from the One-Deflection Model

Here, we shall derive the spectral intensity J in the sharp-edged energy spectrum predicted by the one-deflection model, using the stopping power values from Sec. VI.2A. For simplicity, we assume the surface to be plane, and we shall later in this section discuss the influence of surface roughness.

Figure 7 illustrates the model. The figure shows two collisions, one causing ejection of an Al recoil leaving the surface with energy E, and the other with energy $E-dE$. The depth below the surface for the second collision is $\delta\times dN$ greater than for the first one, where $\delta=2$ Å which is half of the lattice constant, and dN, as seen from Eq. (8), is given by

$$dN=JdE/(iG\eta d\sigma/d\omega). \tag{9}$$

Here, $d\sigma/d\omega$ is the single-collision cross section at energy $T_0'=T_0-R_1\,(dE/dR)_{\mathrm{Ar}}$, see Fig. 7. From the figure it

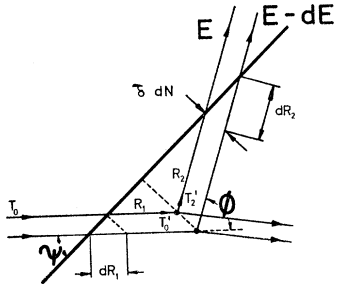

FIG. 7. The one-deflection model for a plane surface, the heavy line. An Ar^+ ion with incident energy T_0 makes a large-angle collision with energy $T_0'=T_0-R_1(dE/dR)_{\mathrm{Ar}}$, and an Al recoil with energy $T_2(\Phi)\times T_0'/T_0$ results. The recoil leaves the surface with energy $E=T_2-R_2(dE/dR)_{\mathrm{Al}}$. Collisions in a region of thickness $\delta\times dN$ (where δ is the distance between {100} planes) contribute to the spectrum in the energy interval $(E,\,E-dE)$.

follows that

$$\delta dN=dR_1\sin\psi=dR_2\sin(\Phi-\psi). \tag{10}$$

The energy difference dE for the two ejected Al recoils is due to a difference in recoil energy dT_2' for the two collisions, and to the energy loss for the difference in recoil path length dR_2 $(dE/dR)_{\mathrm{Al}}$. In the single collision, the recoil energy is proportional to the energy of the incident ion, and therefore dT_2' is given by $dT_2'=dR_1$ $(dE/dR)_{\mathrm{Ar}}T_2/T_0$, where $T_2/T_0=19.3/50$. We thus obtain that dE is given by

$$dE=dR_2\left(\frac{dE}{dR}\right)_{\mathrm{A}}+dR_1\left(\frac{dE}{dR}\right)_{\mathrm{Ar}}\frac{T_2}{T_0}. \tag{11}$$

From Eqs. (9), (10), and (11), one obtains the expression for the spectral intensity as

$$J=\frac{(\eta/\delta)iG(d\sigma/d\omega)}{(dE/dR)_{\mathrm{Al}}\sin^{-1}(\Phi-\psi)+(T_2/T_0)(dE/dR)_{\mathrm{Ar}}\sin^{-1}\psi}. \tag{12}$$

Here, the theoretical cross section $d\sigma/d\omega$ can be obtained when $T_0'=T_0-R_1$ $(dE/dR)_{\mathrm{Ar}}$ is known, that is when R_1 has been found. But R_1 and R_2 are easily calculated because we have constant stopping power values and the recoil energy being proportional to the incident energy in the large-angle collision.

We shall compare the spectral intensities obtained from Eq. (12) for the $\Phi=50°$ cases with $\psi=45°$, 25°, and 5° to the continuum height in the recorded spectra, Fig. 2, and we choose to make the comparison at energy $E=14$ keV. The Ar path length R_1, and the Al path length R_2, both in angstrom units, at $E=14$ keV are found to be

$$\begin{aligned}(R_1,R_2)&=(10.80)\quad\text{with}\quad\psi=45°\\&=(54.54)\quad\text{with}\quad\psi=25°\\&=(119.15)\quad\text{with}\quad\psi=5°\end{aligned} \tag{13}$$

and the theoretical cross section $d\sigma/d\omega$ are increased from the value at $T_0=50$ keV by 0, 2, and 5% for $\psi=45°$, 25°, and 5°, respectively. These cross sections should be inserted in Eq. (12).

The ratios between $J=J_{\mathrm{theor}}$ from Eq. (12) and the recorded continuum height J_{expt} for the $\Phi=50°$ cases at $E=14$ keV, or $E/n=14$ kV, are given in Table II. This table also includes the ratio obtained in a parallel manner for the Ar^+ group in the $\Phi=25°$ spectrum, Fig. 3, where the ratio is taken at $E=35$ keV. It may be noted that the cross section $d\sigma/d\omega$ varies rather slowly with energy both for Al recoils at $\varphi=50°$, and for scattered Ar at $\Theta=25°$. Therefore, the one-deflection model with stopping-power values, which are also constant, predicts a rather constant spectral intensity. The discrepancy in the $\Phi=25°$ case has been discussed in Sec. VI 1.

The influence of multiple scattering, which is neglected in the theoretical model, is particularly compli-

TABLE II. Comparison between the spectral intensity J_{theor} deduced from the one-deflection model, and the experimental intensity J_{expt} which is based on the continuum interpretation also given in the table.

Φ,ψ	J_{theor}/J_{expt}	Continuum interpretation Al recoils	Continuum interpretation Reflected Ar
50°,45°	3.2 } for Al recoils		
50°,25°	1.4 } leaving the	Al^+	no
50°, 5°	0.4 } surface with $E=14$ keV for reflected		
25°,22°	1.4 Ar ions leaving the surface with $E=35$ keV	Al^{2+}	Ar^+

cated when $\Phi-\psi$ or ψ is a small angle, and thus the better case for comparison is the case where $(\Phi,\psi)=(50°,25°)$.

We simplified the one-deflection model by assuming a plane surface, and we shall examine the influence of surface roughness. In the plane-surface case, it is seen that the difference dT_2' in recoil energy for the two collisions is small compared to dR_2 $(dE/dR)_{Al}$ if the second term in the denominator in Eq. (12) is small compared to the first term; this is the case when $\psi \gtrsim \frac{1}{2}\Phi$. With $dT_2'=0$, the value of dR_2 corresponding to dE is the same as if stopping of the incident Ar^+ ion was neglected, and we may assume, for $\psi \gtrsim \frac{1}{2}\Phi$, that dR_2 is the same for all parts of the observed surface also when the surface is not plane. This case should now be considered. The collisions yielding to the spectrum in the interval $(E, E-dE)$ are collisions having a recoil path length between R_2 and R_2+dR_2. It is further seen that, because dR_2 is constant, the corresponding target volume is the same as for a plane surface, and this means that Eq. (12) needs no correction. The argument holds whether the whole surface is visible as observed from the analyzer, or not. When ψ is small, however, it can be shown that the spectral intensity deduced from the one-deflection model depends sensitively on the shape of the surface, and we do not know the surface structure. It may be mentioned that an investigation of surface structures after ion bombardment was performed by Fluit and Datz,[7] who examined irradiated single crystals of Cu. They found ridge-like structures depending on crystallographic directions and on the direction of beam incidence, and the dimensions along the surface were comparable to the range of the incoming ions.

The discussion justifies to some degree the comparison in the case with $(\Phi,\psi)=(50°,25°)$, and here the ratio $J_{theor}/J_{expt}=1.4$ at $E/n=14$ kV shows a fair agreement. The continuum was assumed to contain Al^+ ions only, and if some of the recoils, escaping the surface with energy 14 keV, are neutrals, Al^{2+} and Al^{3+} ions, it follows that the experimental intensity J_{expt} has been underestimated. A higher value of J_{expt} would improve the agreement.

C. Validity of the One-Deflection Model

Many small-angle deflections do take place, and as we consider bigger and bigger deflections, we may ask: When do the deflections become rare events? We may examine this question, using Lindhard's cross sections and assuming random distribution of target atoms. Let us again consider the case with $(\Phi,\psi)=(50°,25°)$. At $E=14$ keV, it is seen from Eq. (13) that the Ar and Al path length are both 54 Å, and this is the mean free path for collisions with impact parameters p smaller than 0.31 Å. For 50-keV Ar, it is computed that the deflection for $p=0.31$ Å is $\Theta=4.1°$. Thus, the mean free path for collisions with $\Theta \geq 4.1°$ is $\lambda_{Ar}(4.1°)=54$ Å. In the Ar on Al collision with $\varphi=50°$, the Ar deflection is $\Theta=31°$ which is considerably bigger than the limit 4.1° for rare events. For 19.3-keV Al, it is calculated that $\Theta \geq 7.8°$ gives 54 Å as the free mean path, $\lambda_{Al}(7.8°)=54$ Å. We estimate that the angles 4.1° for Ar and 7.8° for Al typifies the angular straggling due to small-angle scattering.

From the function $T_2(\varphi)$ shown in Fig. 4 it is derived that the recoil energy in a collision with $\varphi=50°-\Delta\varphi$ is given by

$$T_2(50°-\Delta\varphi)=T_2(50°)+\Delta\varphi(0.83\ \text{keV/degree}). \quad (14)$$

It is seen by inserting the estimates for angular straggling that even collisions with Ar and Al path length about 50 Å may contribute to the spectrum at E/n ratios higher than the position of the Al^+ peak. We may estimate, however, that this smearing out does not prevent the one-deflection model from giving a fair result at $E/n=14$ kV, where the comparison J_{theor} to J_{expt} was made. Here, essentially collisions with $\varphi \approx 50°$ accounts for the particle ejection.

D. Peak Formation

We shall finally make a few comments on the peak formation. Even without a detailed knowledge of the partial spectra for Al^+, Al^{2+}, and Al^{3+}, it is evident from the recorded spectra that the energy spectrum for the ejected Al ions has a peak at the recoil energy for a 50-keV single collision. This spectrum should be formed by summation of the energy spectra for Al^+, Al^{2+}, and Al^{3+}, and it is seen that such a summation would give a spectrum with a sharp, symmetric peak. The existence of this peak is not predicted by the one-deflection model, and an attempt to explain the peak formation must be based on multiple scattering phenomena. From Eq. (14), it is seen that a deviation $\Delta T_2=0.83$ keV in recoil energy in the collision with $\varphi=50°-\Delta\varphi$ corresponds to the $\Delta\varphi=1°$, and here $\Delta T_2/T_2=0.83/19.3=4.3\%$ which is about the recorded half-peak width. Thus, a contribution to the spectrum outside the

[7] J. M. Fluit and S. Datz, Physica **30**, 345 (1964).

peak is obtained for $|\Delta\varphi| > 0.5°$. It has been calculated that $\lambda_{Al}(0.5°) = 4.4$ Å, and that $\lambda_{Al}(1°) = 7.8$ Å, and $\lambda_{Al}(3°) = 20$ Å. It is seen that $\lambda_{Al}(0.5°)$ is of the same order of magnitude as the recoil path length for a collision occurring in the depth $\delta = 2$ Å, that is in the second layer. It is noted that $\lambda_{Al}(\Theta)$ was derived from a random distribution of target atoms, and using the picture with a random distribution below a plane surface, one would not expect a sharp symmetric peak, but a peak with a low-energy tail. For instance, it is seen that a recoil path length of 7.8 Å corresponds to a broadening of the spectrum contribution of about twice the recorded half-peak width, and the contribution is, because of stopping of the incoming and outgoing particle, displaced to lower energies by about 0.8 keV, which is equal to the half-peak width. It is seen that, in order to obtain a symmetric peak, the broadening should increase more abruptly.

Also the experimental result that peak positions do not depend on the angle ψ, Sec. IV.2, is surprising as seen from the following estimate of small-angle deflections in secondary collisions. Let us consider the 19.3-keV Al recoils at $\Phi = 50°$. A deflection of for instance 0.5° in a collision with a neighbor target atom corresponds to the impact parameter 1.1 Å. The energy loss in this weak collision is small compared to the increase in recoil energy for the main collision by changing the recoil angle from 50° to 49.5°. We should therefore obtain a smaller Q value than for the pure single collision, and the effect is quite substantial; the error of 0.5° in the recoil angle gives rise to an error of 390 eV in the Q value. (With a perfect lattice layer as surface, this might in fact provide a tool for studying differential cross sections for small deflections; the angles Φ and ψ select impact parameters in the secondary collisions.) As pointed out, however, the effect was not found.

The explanation of the formation of sharp peaks at positions which do not depend on ψ must be either that the Thomas-Fermi type potential, which we are using, is not a good approximation at impact parameters about 1 Å, or the particular surface conditions must account for it. (If, for instance, the surface is rough on an atomic scale, only recoils from the upper parts of the rough surface may contribute to the sharp peak.)

Whatever the explanation is, the constancy of the peak positions may suggest that the peaks correspond to collisions with recoil angle $\varphi = \Phi$, which means that the deflection resulting from secondary collisions is either negligible or a small deflection perpendicular to the beam-analyzer plane. We do not know the actual surface structure, but we may suggest that the Q values are still considered as single-collision data.

VII. CONCLUDING REMARKS

The data obtained with the highest accuracy were the peak positions from which Q values were derived. The results were $Q = 450$ eV for the Ar on Al collision with the distance of closest approach r_0 in the range 0.12 to 0.18 Å, and higher values for r_0 approaching 0.10 Å. The discussion in Sec. VI2D supports the assumption that the peaks are caused by pure single collisions. The possibility of using solid targets evidently extends the field for single-collision studies.

The spectra were explained on the basis of the knowledge of large-angle collisions, and on theory for heavy-ion penetration, and the absolute measurements of spectral intensities made it possible to check the theoretical model quantitatively. The spectra are discussed rather extensively, partly as an examination as to whether the Q values could be ascribed to single collisions (and we arrived at the answer: probably yes), but also because this type of experiment may yield information on penetration phenomena. It is, for instance, noted that, when the one-deflection model is adequate, the analysis of particles ejected in a particular direction is, in some sense, equivalent to a series of foil transmission experiments with a covered range of foil thickness starting from zero.

ACKNOWLEDGMENTS

The authors are much indebted to Professor E. Everhart and to Professor A. Russek for stimulating interest in this work and for useful discussions. The facilities and equipment of Professor Everhart's laboratory have been freely used in this study. One of us (P.D.) further expresses thanks to the group at this laboratory for hospitality; he wishes also to thank Professor S. K. Allison for valuable discussion and for hospitality during a stay at the Enrico Fermi Institute in Chicago. P. Dahl also expresses his gratitude for an O.E.C.D. stipend.